High-Performance and Thermostable Mica/Cellulose Composite Paper for Sustainable Packaging Applications

Chenqiao Li,[a] Na Wang,[a] Shan Wu,[a] Jiahao Shen,[b] Chen Zhou,[b] Suxia Hu,[a] Weiping Jia,[a] Wenting Liu,[a,] * Zhangang Cheng,[a] Guoxi Xiong,[a] Bo Wang,[a] and Qinghua Feng [b,]*

*Corresponding author: liuwt@hbtobacco.cn (W.L.); fqhpaper@163.com (Q.F.)

DOI: 10.15376/biores.21.3.6713-6725

GRAPHICAL ABSTRACT

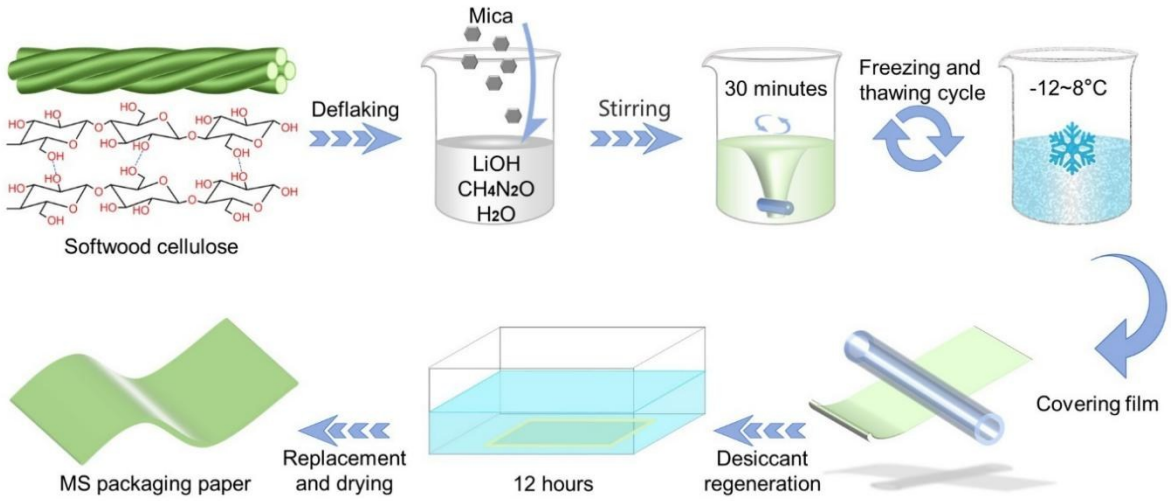

High-Performance and Thermostable Mica/Cellulose Composite Paper for Sustainable Packaging Applications

Chenqiao Li,[a] Na Wang,[a] Shan Wu,[a] Jiahao Shen,[b] Chen Zhou,[b] Suxia Hu,[a] Weiping Jia,[a] Wenting Liu,[a,*] Zhangang Cheng,[a] Guoxi Xiong,[a] Bo Wang,[a] and Qinghua Feng [b,*]

In this study, high-performance packaging paper was developed by dissolving softwood cellulose in a LiOH/urea system and incorporating nano-mica to enhance its mechanical properties and thermal stability. Characterization by scanning electron microscopy (SEM), X-ray diffraction (XRD), and Fourier transform infrared spectroscopy (FT-IR) confirmed partial crystalline transformation in the regenerated cellulose films. Mechanical testing showed that the composite film with 10% mica exhibited a tensile strength of 87.69 MPa and a modulus of 6.82 GPa, demonstrating excellent tensile strength, rigidity, and tear resistance, making it suitable for high-strength packaging applications. Thermogravimetric analysis revealed that the composite paper underwent major thermal degradation at approximately 350 °C, offering superior thermal stability over conventional cellulose-based packaging materials, making it ideal for industrial and electronic component packaging. This study successfully developed a sustainable, high-performance packaging material through the synergistic effects of nanocellulose and nano-mica, providing new insights for advanced cellulose-based packaging solutions.

DOI: 10.15376/biores.21.3.6713-6725

Keywords: Cellulose I/II; Mica; Mica-cellulose composites; Packing material

*Contact information: a: Technology R&D Center, China Tobacco Hubei Industrial Corporation, Wuhan, 430040, China; b: Hubei Provincial Key Laboratory of Green Materials for Light Industry, New Materials and Green Manufacturing Talent Introduction and Innovation Demonstration Base. Hubei University of Technology, Wuhan 430068, China; *Corresponding author: liuwt@hbtobacco.cn (W.L.); fqhpaper@163.com (Q.F.)*

INTRODUCTION

With the growing global demand for sustainable packaging materials, the packaging industry is facing the challenge of transitioning from traditional plastics to environmentally friendly alternatives (Adel *et al.* 2021; Jiao *et al.* 2021). While plastic packaging offers excellent barrier properties and mechanical performance, its non-degradability has led to severe environmental pollution. Therefore, the search for biodegradable, renewable, and eco-friendly packaging materials with superior mechanical properties has become a key focus of current research (Bangar *et al.* 2022; Kwak *et al.* 2023).

Natural cellulose, as a widely available material in the natural ecosystem, is recognized for its renewability and biodegradability, making it a traditional paper-based packaging material for applications such as food packaging, express delivery packaging, and electronic product packaging (Yi *et al.* 2022; Niu *et al.* 2024). However, conventional

cellulose-based packaging materials still face several challenges: compared to plastics, ordinary paper exhibits lower tear resistance, fold endurance, and puncture resistance (Martín-Sampedro *et al.* 2022; Lay *et al.* 2023; Sanchez-Salvador *et al.* 2023), making it difficult to meet the demands of high-performance packaging; cellulose paper tends to absorb moisture and soften in humid environments, leading to structural damage; and at high temperatures, cellulose undergoes thermal degradation, limiting its applicability in specialized packaging scenarios such as heat-resistant food packaging and electronic component packaging (Barbash *et al.* 2022; Shankar *et al.* 2023; Song *et al.* 2024).

Nanomaterials have flourished in various production fields. Against this backdrop, theoretical research on the nanonization of natural cellulose and its practical applications has become increasingly mature (Chen *et al.* 2021; Perdoch *et al.* 2022; Lourenço *et al.* 2023). Compared to natural cellulose, nanocellulose exhibits a higher specific surface area, stronger hydrogen bonding interactions, and a denser network structure, enabling it to bind more effectively with the matrix in composite materials, films, and coatings, thereby significantly enhancing the overall performance of materials and partially overcoming the inherent limitations of cellulose (Wang *et al.* 2024; Zhang *et al.* 2024). In the exploration of how to efficiently utilize nanocellulose to enhance paper properties, numerous studies have been conducted. For example, researchers have prepared cotton cellulose nanofibers through ultrasonic treatment combined with deep eutectic solvent (DES) pretreatment and obtained paper with enhanced mechanical properties (Deng *et al.* 2022). Additionally, fillers have been used to improve the environmental adaptability of paper, such as using aluminum trihydrate fillers to enhance the strength of cellulose paper subjected to high-temperature treatment (Chen *et al.* 2011). The incorporation of nanocellulose has also been shown to modify the electrical properties of insulating paper while simultaneously providing higher modulus (Zhai *et al.* 2024). Furthermore, chemical modification can impart special properties to nanocellulose, such as the preparation of nanocellulose-based hydrophobic coatings through chemical modification, which can be applied to superhydrophobic coated paper for food packaging (Li *et al.* 2023).

Mica, a widely abundant layered silicate mineral in nature, possesses a platelet structure, excellent chemical inertness, electrical insulation, and thermal stability, making it a widely used filler in applications such as electronic materials, composites, barrier coatings, and flame-retardant materials (Pan *et al.* 2023). Through exfoliation, nano-mica with a high aspect ratio can be obtained. As a reinforcing filler, nano-mica can significantly enhance the mechanical strength, thermal stability, and barrier properties of polymers such as polyvinyl alcohol (PVA), polylactic acid (PLA), and polyurethane (PU), as well as rubber. In recent years, reports on the successful combination of nano-mica and cellulose for the fabrication of multifunctional paper have emerged (Niu *et al.* 2021; Santos *et al.* 2023; Wang *et al.* 2023). For instance, biosynthesized bacterial cellulose/mica nanopaper has demonstrated excellent mechanical and electrical insulation properties (Sun *et al.* 2023); a novel double-network mica-based composite film, prepared by introducing aramid nanofibers (ANF) and nanofibrillated cellulose (NFC), has exhibited remarkable dielectric performance under high-temperature conditions (Wang *et al.* 2022). These studies have provided valuable insights into present research.

In this study, softwood cellulose was dissolved in a LiOH/urea system and combined with nano-mica to develop a novel high-performance packaging paper. Nanocellulose effectively enhances the strength and toughness of the paper, while the incorporation of nano-mica significantly improves its barrier properties and thermal stability. As two important nanomaterials, nano-mica and nanocellulose offer superior

mechanical performance and environmental stability, providing a promising strategy for the development of next-generation high-performance packaging materials.

EXPERIMENTAL

Materials

Softwood dissolving pulp (DP = 450) was provided by Hongyang New Material Technology Co., Ltd. (Dangyang, China); Mica was supplied by Hubei Pingan Electrical Technology Co., Ltd. LiOH, urea, and ethanol were purchased from Sinopharm Chemical Reagent Co., Ltd. Deionized water was prepared in the laboratory.

Preparation of MC Films Treated with LiOH/thiourea Aqueous Solution

The softwood pulp board was initially dispersed using a stirrer, followed by sheet formation and drying for later use (sheet former model: Rapid Köthen sheet former, RK-3A, Frank-PTI). Four grams of mica was added to 100 g of deionized water under stirring and subjected to centrifugation for 5 min at 500 rpm (Fig. 1). The supernatant was collected and centrifuged again for 5 min at 5000 rpm. The sediment from the second centrifugation was dried and used as the nano-mica raw material. The size distribution of the obtained nano-mica is shown in Fig. S1. A 100 g LiOH/urea/water solution was prepared in a ratio of 4.2:12:83.8, into which a predetermined amount of nano-mica was added and stirred for 30 min. Then, 4 g of softwood cellulose paper was introduced into the mixture and stirred for 1 hour. The resulting mixture underwent three freeze-thaw cycles (freezing at -12 °C, thawing at 8 °C) to achieve complete cellulose dissolution. To remove air bubbles, the solution was centrifuged at 7500 rpm for 5 min, then cast onto a glass plate. A quartz tube was used to spread the mixture into a 1 mm-thick film, which was subsequently transferred to a regeneration bath composed of an ethanol-to-water ratio of 2:3 and treated for 12 h. The film was repeatedly washed with deionized water to remove residual reagents. Finally, the film was vacuum-dried in the paper machine drying zone at 97 °C under -10 kPa pressure. All prepared samples were stored in sealed bags for future use.

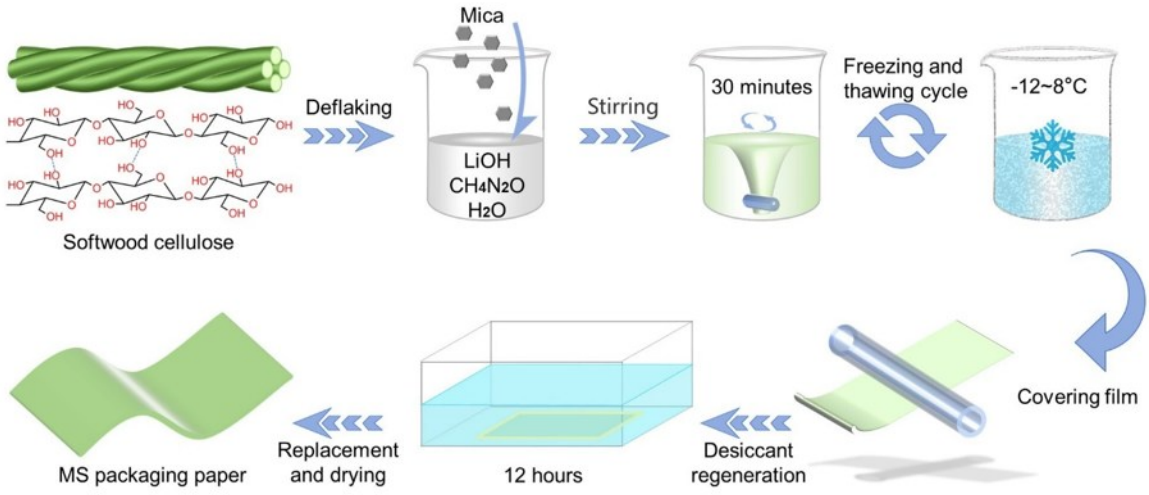

Fig. 1. Schematic illustration of the process for dissolving softwood cellulose using the LiOH/urea system and its combination with nano-mica to fabricate high-performance packaging paper

SEM Analysis

The cross-section images of the films were observed using an ultra-high resolution cold field scanning electron microscope (SU8010, HITACHI Ltd., Japan) operated at an accelerating voltage of 5 kV. Before imaging, the films were dried in the dryer section of the former sheet, and then the films were coated with gold using the SEM sputter coater (MC1000; HITACHI Ltd., Japan) to improve the paper's electric conductivity. For the cross-section images, they were cut into strips measuring 10 cm in length and 0.5 cm in width using a paper cutter.

FT-IR Spectroscopy Analysis

The chemical structures of raw materials and film samples were determined by an FT-IR spectrometer (Thermo Fisher Scientific Inc., USA). The scanning range of the samples was set to 650-4000 cm^{-1}, and the number of scans was 16 times with a resolution of 4 cm^{-1}.

XRD Analysis

The crystal structure of the C and MC films was identified using polycrystalline X-ray diffraction (Empyrean, PANalytical B.V., Netherlands). The Cu Kα radiation generated at 45 kV and 40 mA was irradiated on the surface of the samples. Scans were taken over a 2θ range from 5 to 40° at a scanning speed of 5°/ min.

The crystalline degree (XC) was calculated by Eq. 1,

$$X_C = Acr/(Aam+Acr) * 100, \quad (1)$$

where *Acr* and *Aam* are the integrated area of the crystal line and the amorphous phases, respectively.

Tensile Tests

The mechanical strength of the film was tested using a universal testing machine equipped with a 1 kN load cell. The detailed sample compositions and the number of specimens tested per group are listed in Table S1. The tensile test was conducted at a stretching speed of 10 mm/min, with a gauge length of 50 mm. The specimen had a length of 100 mm and a width of 5 mm. The film thickness was measured using a computer-controlled thickness densitometer. The measured data were plotted as a stress-strain curve using Origin software to visually and concisely represent the mechanical properties of the specimen.

Thermostability of the Films

The thermal properties of the film were tested by TA-Q500 thermogravimetric analyzer (Q500, TA, USA). The samples were heated from 80 °C to 800 °C at a rate of 10°C /min in the N_2 atmosphere (Wang *et al*. 2022).

RESULTS AND DISCUSSION

Morphology Analysis

The LiOH/urea system effectively disrupts the hydrogen bonds between cellulose molecules at low temperatures, promoting hydration and swelling (Shen *et al.* 2024). Under

this system, the amorphous regions of cellulose are dissolved first, while the crystalline regions, particularly the cellulose I structure, are partially disrupted, causing the fiber structure to loosen and reducing the intermolecular interactions between the cellulose chains (Gan *et al.* 2023). This creates favorable conditions for subsequent cellulose reorganization. After dissolution, as the solvent is removed, cellulose undergoes regeneration, forming a new fiber network. During this process, cellulose may transition from its original cellulose I crystalline structure to cellulose II, accompanied by a rearrangement of the hydrogen bond network. From the cross-sectional images of samples with mica content ranging from 0% to 10% in Fig. 2, at 0% mica content, the cross-section exhibits distinctly loose-arranged cork-like cellulose fibers with significant inter-fiber gaps and irregular voids. When mica content increased to 2%, mica flakes began to embed within the fibers, resulting in slightly reduced pore sizes. At 5% mica content, the fiber structure became partially obscured while mica demonstrated enhanced continuity. Upon reaching 10% mica content, the original fiber morphology was almost entirely replaced by a dense, uniform composite structure—where mica nanosheets were uniformly dispersed and horizontally aligned, significantly reducing porosity compared to the original pulp film. This progressive densification and alignment of mica nanosheets not only improved the spatial uniformity of the film but also enhanced stress transfer efficiency through the dense structure and interfacial bonding between cellulose and mica. This helps improve the uniformity and mechanical properties of the film. Compared to randomly distributed inorganic fillers, the horizontally aligned nano-mica platelets (with an aspect ratio of 60.33) in the cross-section can more evenly bear and transfer loads, thereby reducing material brittleness while improving toughness and tensile strength. Additionally, the alignment of the mica nano-plates reduces interfacial scattering, allowing the film to maintain a high level of transparency, which meets the aesthetic requirements for packaging paper (Li *et al.* 2022).

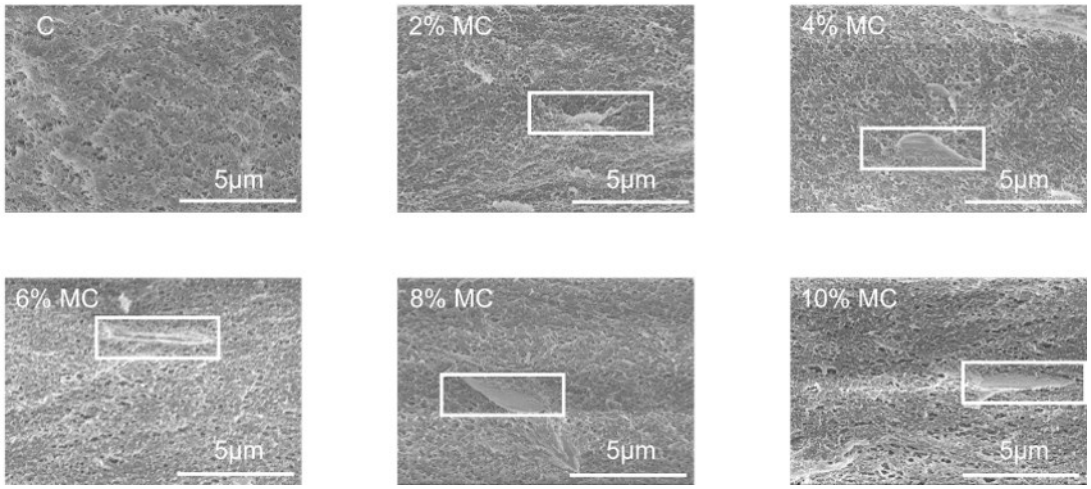

Fig. 2. Cross-sectional electron microscope images of pure softwood nanocellulose films and mica/cellulose composite films with 2 to 10% mica content

FT-IR and XRD Pattern Analysis

Figure 3 shows that the infrared characteristic peaks of pure cellulose paper were largely consistent with those of cellulose films treated with the LiOH/urea system and MC composite films. Natural cellulose predominantly exists in the cellulose I form; however,

after dissolution and regeneration in solution, it can transform into the more thermodynamically stable cellulose II structure. The cellulose films and MC composite films treated with the LiOH/urea system exhibited characteristic peaks at 1426 cm^{-1} and 1115 cm^{-1}, indicating the presence of cellulose I. However, the intensity of these peaks was lower than that of untreated softwood paper, suggesting that a portion of the cellulose within the membrane samples underwent a crystalline transformation from cellulose I to cellulose II upon treatment with the LiOH/urea system.

By comparing the XRD patterns of pure softwood paper, mica powder, regenerated cellulose films, and MC composite films, it is evident that the cellulose within softwood paper exhibits a typical cellulose I crystalline structure, with diffraction peaks appearing at 2θ = 14.9°, 16.6°, and 22.6°, corresponding to the (110), (1-10), and (002) crystal planes, respectively (Shen *et al*. 2023). The regenerated cellulose films and MC composite films also exhibited similar diffraction peaks, although with lower peak intensities than softwood paper. Quantitative analysis showed that the crystallinity of regenerated cellulose films and MC composite films were 42.9%, significantly lower than the 67.3% of softwood paper.

For mica, distinct diffraction peaks were observed at 2θ = 8.8°, 17.8°, 26.9°, and 36.1°, corresponding to the (001) plane, the second-order derivative peak of the (001) plane, the (003) plane, and the (005) plane, respectively. The 10% MC composite film exhibited diffraction peaks that aligned closely with those of mica. The XRD analysis further confirms that, after treatment with the LiOH/urea system, part of the cellulose underwent a crystalline transformation from cellulose I to cellulose II. Additionally, the results indicate a strong interaction between mica and the treated cellulose, demonstrating successful integration within the composite structure (Zhou *et al*. 2025).

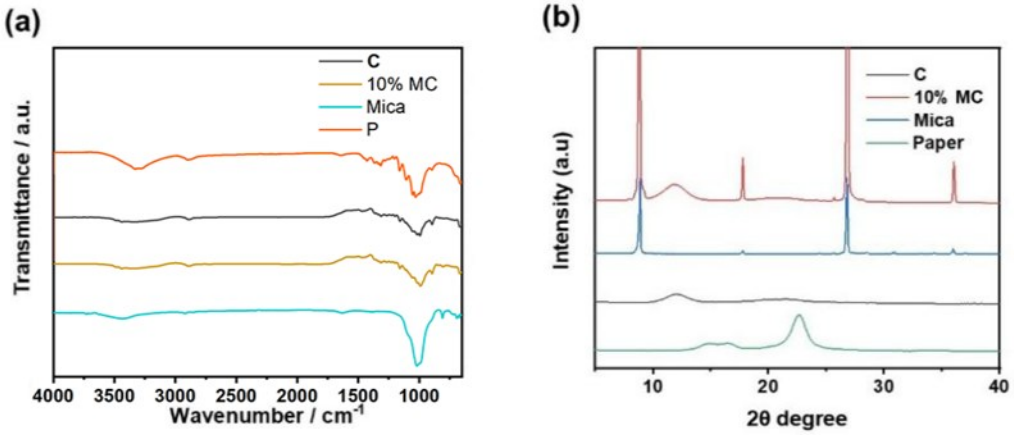

Fig. 3. (a) Infrared spectra of pure cellulose paper, pure cellulose film, and MC composite films with 10% mica content; (b) XRD patterns of pure cellulose paper, pure cellulose film, and MC composite film with 10% mica content.

Mechanical Performance Analysis

Figure 4a shows that with the increase in mica content, the tensile strength of the MC composite film significantly improved, reaching a maximum value of 87.69 MPa when the mica content was 10%. The addition of a small amount of mica greatly enhanced the tensile strength of the cellulose film, suggesting that MC composite films have considerable potential for applications in the packaging industry. Although the impact of mica on the toughness of the cellulose film is limited, the improvement in the modulus of the mica-cellulose films is quite significant, providing the film with strong rigidity and resistance to deformation (Jiang and Wang. 2022; Harada *et al.* 2023). This enhances the

film's ability to resist tearing when subjected to tensile or puncture forces, thereby improving the protective and safety performance of the packaging, which compensates for the inherent limitations of traditional cellulose films (Fig. 4b, c).

Figure 5 presents a simulation of the deformation and eventual fracture process of the MC composite film under high tensile forces. After the film underwent regeneration and was dried, mica nanoparticles interacted with cellulose *via* hydrogen bonding and electrostatic forces, strengthening the connections between fibers and making the internal structure of the paper denser and less prone to breakage (Sharifi *et al.* 2022; Yeamsuksawat *et al.* 2022; Yuan *et al.* 2023). Due to the high aspect ratio (plate-like structure) of mica nanoparticles, they can align laterally within the paper, filling the voids between cellulose fibers, which increases the overall density and uniformity of the material. When the paper experiences tearing, the mica nanoparticles can help distribute stress and prevent crack propagation, making the material more resistant to tearing. This enhanced stress distribution and crack arresting mechanism not only improve the mechanical strength of the film but also contribute to its long-term durability and stability under various stress conditions. These attributes make mica-cellulose films a promising material for high-performance packaging applications.

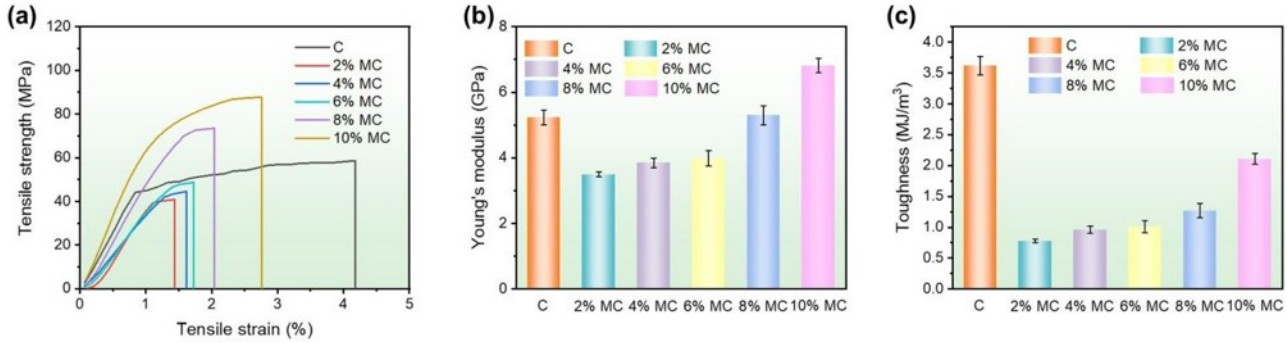

Fig. 4. (a) Tensile strength comparison of pure cellulose film and MC composite films with 2 to 10% mica content; (b) modulus and (c) toughness of pure cellulose film and MC composite films with 2 to 10% mica content.

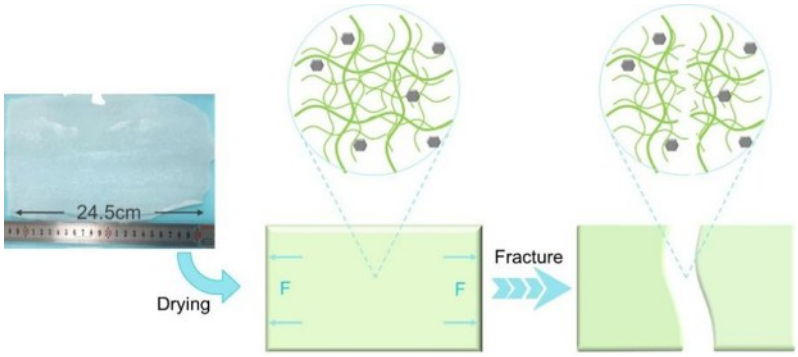

Fig. 5. Tensile fracture model of MC composite film

Thermal Stability Analysis

It can be observed that mica exhibits almost no decomposition under high-temperature conditions, demonstrating excellent thermal stability. As the mica content increased, the amount of residual solid material in the film samples after high-temperature treatment significantly increased. Specifically, the final solid mass of pure cellulose films was in a ratio of 1:5.17 compared to the residual solid mass after removing mica in the 10%

MC composite film. This further indicates that the lateral arrangement of mica nanosheets in the film forms a physical barrier, providing thermal insulation and successfully promoting the conversion of cellulose into stable carbon residues rather than completely decomposing into gaseous products (as shown in Fig. 6a). According to the differential thermal gravity (DTG) curve, all film samples undergo rapid thermal degradation around 350 °C, proving that regenerated cellulose retains a high degree of crystallinity (Kim *et al.* 2022; Mai *et al.* 2023; Sanchez-Salvador *et al.* 2023). This phenomenon macroscopically indicates that the prepared MC composite films possess good thermal stability in high-temperature environments, making them suitable for applications in higher temperature conditions, and thus maintaining excellent performance as packaging materials (Fig. 6b). This thermal stability enhances the adaptability of mica-cellulose films in practical applications, especially in packaging materials that require high-temperature resistance (Guan *et al.* 2021; Jiang *et al.* 2021).

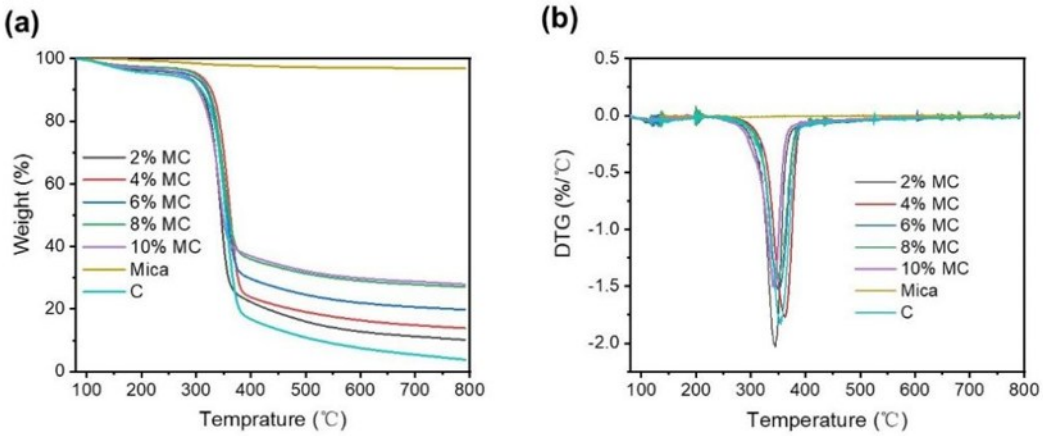

Fig. 6. TG (a) and DTG (b) of pure cellulose membrane and MC composite membrane with 0 to 10 % mica content

CONCLUSIONS

1. This study conducted a detailed investigation of the crystalline phase transition of cellulose in solution-regenerated film samples using scanning electron microscopy (SEM), X-ray diffraction (XRD), and Fourier transform infrared spectroscopy (FT-IR).
2. Through tensile testing, the composite film sample with 10% mica content exhibited a high tensile strength of 87.69 MPa and a high modulus of 6.82 GPa. The paper prepared by combining a small amount of mica with cellulose demonstrated excellent mechanical properties, including high tensile strength, rigidity, and tear resistance, making it highly suitable for packaging materials. This composite paper possesses good uniformity and density, not only providing outstanding mechanical support but also enhancing protection and durability in packaging applications.
3. The thermogravimetric analysis results of the composite sample indicate that significant thermal degradation occurs at approximately 350 °C, demonstrating excellent thermal stability. Compared to traditional cellulose-based packaging materials, this composite paper can be utilized in more demanding application environments, such as industrial packaging and electronic component packaging, while maintaining stable physical properties even under high-temperature conditions.

ACKNOWLEDGMENTS

The authors are grateful to the Key R & D Program of Hubei Province (2022BAD026).

REFERENCES CITED

Adel, A. M., Al-Shemy, M. T., Diab, M. A., El-Sakhawy, M., Toro, R. G., Montanari, R., de Caro, T., and Caschera, D. (2021). "Fabrication of packaging paper sheets decorated with alginate/oxidized nanocellulose-silver nanoparticles bio-nanocomposite," *International Journal of Biological Macromolecules* 181, 612-620. https://doi.org/10.1016/j.ijbiomac.2021.03.182

Bangar, S. P., Harussani, M. M., Ilyas, R. A., Ashogbon, A. O., Singh, A., Trif, M., and Jafari, S. M. (2022). "Surface modifications of cellulose nanocrystals: Processes, properties, and applications," *Food Hydrocolloids* 130, 107689. https://doi.org/10.1016/j.foodhyd.2022.107689

Barbash, V. A., Yashchenko, O. V., Yakymenko, O. S., Zakharko, R. M., and Myshak, V. D. (2022). "Preparation of hemp nanocellulose and its use to improve the properties of paper for food packaging," *Cellulose* 29(15), 8305-8317. https://doi.org/10.1007/s10570-022-04773-6

Chen, H., Chen, K., Yang, R., Yang, F., and Gao, W. (2011). "Use of aluminum trihydrate filler to improve the strength properties of cellulosic paper exposed to high temperature treatment," *BioResources* 6(3), 2399-2410. https://doi.org/10.15376/biores.6.3.2399-2410

Chen, S., Chen, Y., Li, D., Xu, Y., and Xu, F. (2021). "Flexible and sensitivity-adjustable pressure sensors based on carbonized bacterial nanocellulose/wood-derived cellulose nanofibril composite aerogels," *ACS Applied Materials & Interfaces* 13(7), 8754-8763. https://doi.org/10.1021/acsami.0c21392

Deng, X., Wan, L., Sun, H., Li, C., Liu, F., Yan, X., Liu, K., and Ye, S. (2022). "Preparation of nanocellulose from cotton fibers in deep eutectic solvent (DES) and its application in paper," *BioResources* 17(1), 714-724. https://doi.org/10.15376/biores.17.1.714-724

Guan, Q.-F., Yang, H.-B., Yin, C.-H., Han, Z.-M., Yang, K.-P., Ling, Z.-C., and Yu, S.-H. (2021). "Nacre-inspired sustainable coatings with remarkable fire-retardant and energy-saving cooling performance," *ACS Materials Letters* 3(2), 243-248. https://doi.org/10.1021/acsmaterialslett.0c00509

Gan, M., Tian, L., Chen, Y., Xin, J., Si, H., Xie, Y., and Feng, Q. (2023). "All-cellulose composites fabricated by *in-situ* welding," *BioResources* 18(2), 3044-3055. https://doi.org/10.15376/biores.18.2.3044-3055

Harada, K., Chu, P., Xu, K., Fujimori, A. (2023). "Polypropylene-based nanocomposite with improved mechanical properties: Effect of cellulose nanofiber and polyrotaxane with partial miscibility," *Polymer Composites* 44(5), 2977-2987. https://doi.org/10.1002/pc.27295

Jiang, H., Jiang, L., Zhang, P., Zhang, X., Ma, N., and Wei, H. (2021). "Force-induced self-assembly of supramolecular modified mica nanosheets for ductile and heat-resistant mica papers," *Langmuir* 37(17), 5131-5138. https://doi.org/10.1021/acs.langmuir.1c00001

Jiang, K., and Wang, X. (2022). "Preparation and application of maleic acid crosslinked

polyvinyl alcohol/mica coating for barrier paper," *Progress in Organic Coatings* 170, 106937. https://doi.org/10.1016/j.porgcoat.2022.106937

Jiao, D., Lossada, F., Guo, J., Skarsetz, O., Hoenders, D., Liu, J., and Walther, A. (2021). "Electrical switching of high-performance bioinspired nanocellulose nanocomposites," *Nature Communications* 12(1), 1312. https://doi.org/10.1038/s41467-021-21599-1

Kim, S.-W., Lee, K.-H., Lee, Y.-H., Youe, W.-J., Gwon, J.-G., and Lee, S.-Y. (2022). "Transparent and multi-foldable nanocellulose paper microsupercapacitors," *Advanced Science* 9(34), 2203720. https://doi.org/10.1002/advs.202203720

Kwak, H., Kim, H., Park, S.-A., Lee, M., Jang, M., Park, S. B., Hwang, S. Y., Kim, H. J., Jeon, H., Koo, J. M., Park, J., and Oh, D. X. (2023). "Biodegradable, water-resistant, anti-fizzing, polyester nanocellulose composite paper straws," *Advanced Science* 10(1), 2205554. https://doi.org/10.1002/advs.202205554

Lay, M., Say, M. G., and Engquist, I. (2023). "Direct ink writing of nanocellulose and PEDOT:PSS for flexible electronic patterned and supercapacitor papers," *Advanced Materials Technologies* 8(18), 2300652. https://doi.org/10.1002/admt.202300652

Li, L., Maddalena, L., Nishiyama, Y., Carosio, F., Ogawa, Y., and Berglund, L. A. (2022). "Recyclable nanocomposites of well-dispersed 2D layered silicates in cellulose nanofibril (CNF) matrix," *Carbohydrate Polymers* 279, 119004. https://doi.org/10.1016/j.carbpol.2021.119004

Li, P., Zhou, M., Jian, B., Lei, H., Liu, R., Zhou, X., Li, X., Wang, Y., and Zhou, B. (2023). "Paper material coated with soybean residue nanocellulose waterproof agent and its application in food packaging," *Industrial Crops and Products* 199, 116749. https://doi.org/10.1016/j.indcrop.2023.116749

Lourenço, A. F., Martins, D., Dourado, F., Sarmento, P., Ferreira, P. J. T., and Gamelas, J. A. F. (2023). "Impact of bacterial cellulose on the physical properties and printing quality of fine papers," *Carbohydrate Polymers* 314, 120915. https://doi.org/10.1016/j.carbpol.2023.120915

Martín-Sampedro, R., Eugenio, M. E., Ibarra, D., Ruiz-Hitzky, E., Aranda, P., and Darder, M. (2022). "Tailoring the properties of nanocellulose-sepiolite hybrid nanopapers by varying the nanocellulose type and clay content," *Cellulose* 29(9), 5265-5287. https://doi.org/10.1007/s10570-022-04565-y

Mai, T., Guo, W.-Y., Wang, P.-L., Chen, L., Qi, M.-Y., Liu, Q., Ding, Y., and Ma, M.-G. (2023). "Bilayer metal-organic frameworks/MXene/nanocellulose paper with electromagnetic double loss for absorption-dominated electromagnetic interference shielding," *Chemical Engineering Journal* 464, 142517. https://doi.org/10.1016/j.cej.2023.142517

Niu, H., Zhang, K., Myllymäki, S., Ismail, M. Y., Kinnunen, P., Illikainen, M., and Liimatainen, H. (2021). "Nanostructured and Advanced designs from biomass and mineral residues: Multifunctional biopolymer hydrogels and hybrid films reinforced with exfoliated mica nanosheets," *ACS Applied Materials & Interfaces* 13(48), 57841-57850. https://doi.org/10.1021/acsami.1c18911

Niu, Z., Wang, Q., Lu, J., Hu, Y., Huang, J., Zhao, W., Liu, Y., Long, Y.-Z., and Han, G. (2024). "Electrospun cellulose nanocrystals reinforced flexible sensing paper for triboelectric energy harvesting and dynamic self-powered tactile perception," *Small* 20(17), 2307810. https://doi.org/10.1002/smll.202307810

Pan, X.-F., Bao, Z., Xu, W., Gao, H.-L., Wu, B., Zhu, Y., Yu, G.-H., Chen, J., Zhang, S.-C., Li, L., Wu, H.-A., Li, X., and Yu, S.-H. (2023). "Recyclable nacre-like aramid-

mica nanopapers with enhanced mechanical and electrical insulating properties," *Advanced Functional Materials* 33(9), 2210901. https://doi.org/10.1002/adfm.202210901

Perdoch, W., Cao, Z., Florczak, P., Markiewicz, R., Jarek, M., Olejnik, K., and Mazela, B. (2022). "Influence of nanocellulose structure on paper reinforcement," *Molecules* 27(15), 4696. https://doi.org/10.3390/molecules27154696

Sharifi, A. R., Naghdi, T., Yousefi, H., Kiani, M. A., and Golmohammadi, H. (2022). "Nanopapers toward green photonic and optical applications," *ACS Sustainable Chemistry & Engineering* 10(51), 16995-17026. https://doi.org/10.1021/acssuschemeng.2c04224

Sanchez-Salvador, J. L., Rasteiro, M. G., Balea, A., Sharma, M., Pedrosa, J. F. S., Negro, C., Monte, M. C., Blanco, A., and Ferreira, P. J. T. (2023). "Influence of dispersion of fibrillated cellulose on the reinforcement of coated papers," *International Journal of Biological Macromolecules* 248, 125886. https://doi.org/10.1016/j.ijbiomac.2023.125886

Santos, J. J., Lopes, J. H., de Aguiar, K. M. F. R., Simões, M. B., M´Peko, J.-C., Jasinevicius, R. G., Cavalheiro, E. T., Imasato, H., and Rodrigues-Filho, U. P. (2023). "Hybrid Bisphenol A non-isocyanate polyurethane composite with Mica powder: A new insulating material," *Journal of CO2 Utilization* 67, 102303. https://doi.org/10.1016/j.jcou.2022.102303

Shankar, A., A.K, A. M., Narayan, R., and Chakrabarty, A. (2023). "Emulsion polymerized styrene acrylic/nanocellulose composite coating to improve the strength and hydrophobicity of kraft paper," *Progress in Organic Coatings* 182, 107634. https://doi.org/10.1016/j.porgcoat.2023.107634

Shen, J., Yang, Y., Yang, Z., Li, J., Li, X., Xie, Y., and Feng, Q. (2024). "All-natural, thermally conductive, flame-retardant electrical insulating lignocellulose-mica composite film fabricated via in-situ mineralization," *Industrial Crops and Products* 220, 119173. https://doi.org/10.1016/j.indcrop.2024.119173

Song, S., Wu, Q., Ji, D., Li, L., Wang, Q., and Zhang, M. (2024). "Nacre-inspired composite paper of PVA crosslinked basalt scale and nanocellulose with enhanced mechanical, electrical insulating and ultraviolet-resistant aging performance," *International Journal of Biological Macromolecules* 257, 128602. https://doi.org/10.1016/j.ijbiomac.2023.128602

Sun, W.-B., Han, Z.-M., Yue, X., Zhang, H.-Y., Yang, K.-P., Liu, Z.-X., Li, D.-H., Zhao, Y.-X., Ling, Z.-C., Yang, H.-B., Guan, Q.-F., and Yu, S.-H. (2023). "Nacre-inspired bacterial cellulose/mica nanopaper with excellent mechanical and electrical insulating properties by biosynthesis," *Advanced Materials* 35(24), 2300241. https://doi.org/10.1002/adma.202300241

Wang, X., Guo, J., Ren, H., Jin, J., He, H., Jin, P., Wu, Z., and Zheng, Y. (2024). "Research progress of nanocellulose-based food packaging," *Trends in Food Science & Technology* 143, 104289. https://doi.org/10.1016/j.tifs.2023.104289

Wang, Y., Dang, W., Yao, C., Tian, C., and Lu, Z. (2022). "Flexible and high-temperature dielectric ANF-NFC/mica@PDA composite film with high breakdown strength," *Journal of Materials Science* 57(43), 20174-20186. https://doi.org/10.1007/s10853-022-07878-2

Wang, Z., Yang, L., Dai, L., Huang, Z., Wu, K., and Liu, B. (2023). "Scalable production of 2D minerals by polymer intercalation and adhesion for multifunctional applications," *Small Methods* 7(9), 2300529. https://doi.org/10.1002/smtd.202300529

Yeamsuksawat, T., Morishita, Y., Shirahama, J., Huang, Y., Kasuga, T., Nogi, M., and Koga, H. (2022). "Semicarbonized subwavelength-nanopore-structured nanocellulose paper for applications in solar thermal heating," *Chemistry of Materials* 34(16), 7379-7388. https://doi.org/10.1021/acs.chemmater.2c01466

Yi, K., Fu, S., and Huang, Y. (2022). "Nanocellulose-based superhydrophobic coating with acid resistance and fluorescence," *Progress in Organic Coatings* 168, 106911. https://doi.org/10.1016/j.porgcoat.2022.106911

Yuan, W., Yuan, H., Jiao, K., Zhu, J., Lim, E. G., Mitrovic, I., Duan, S., Wang, Y., Cong, S., Zhao, C., Sun, J., Liu, X., and Song, P. (2023). "Facile microembossing process for microchannel fabrication for nanocellulose-paper-based microfluidics," *ACS Applied Materials & Interfaces* 15(5), 6420-6430. https://doi.org/10.1021/acsami.2c19354

Zhai, X., Zhang, D., Li, X., Shao, X., Zhang, T., Zhan, J., Zhao, H., Mu, H., and Zhang, G. J. (2024). "Enhancement and prediction of mechanical properties of microcellulose/ nanocellulose-modified insulating paper," *IEEE Transactions on Dielectrics and Electrical Insulation* 31(5), 2642-2651. https://doi.org/10.1109/TDEI.2024.3422159

Zhang, H., Wang, S., Zhang, J., Zhou, G., Sun, X., Wang, Y., Wang, Y., and Zhang, K. (2024). "High-sensitivity piezoresistive sensors based on cellulose handsheets using origami-inspired corrugated structures," *Carbohydrate Polymers* 328, 121742. https://doi.org/10.1016/j.carbpol.2023.121742

Article submitted: March 27, 2025; Peer review completed: June 30, 2025; Revisions accepted: May 29, 2025; Published: June 8, 2026.
DOI: 10.15376/biores.21.3.6713-6725

SUPPLEMENTARY MATERIALS

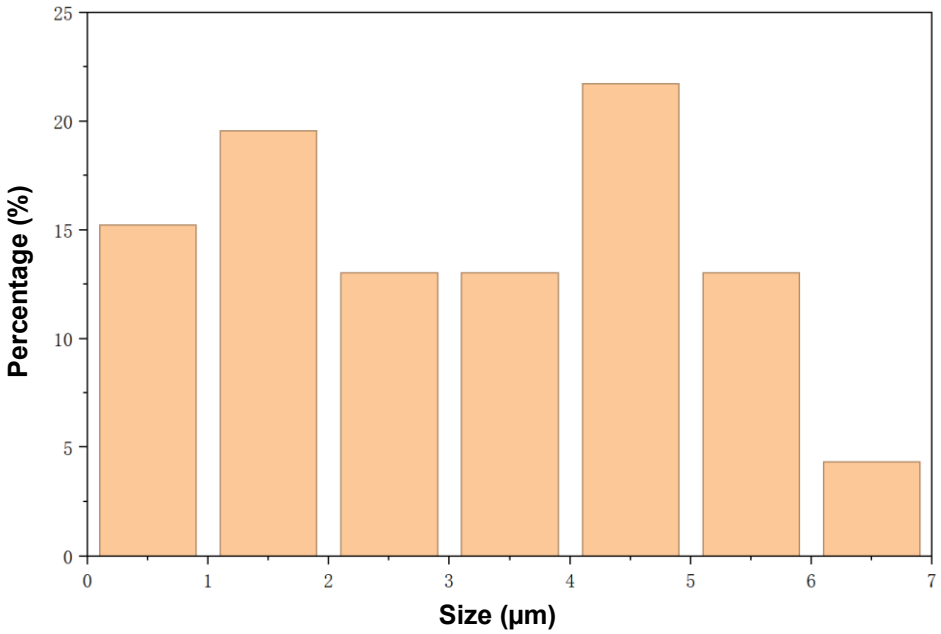

Fig. S1. Size distribution size of mica

Table S1. Mica Ratio and Tensile Test Standard

Sample	Mica amount (w%)	Tensile Test Standard	Number of Tensile Test
C	0	ASTM D882-18	5
2%MC	2	ASTM D882-18	5
4%MC	4	ASTM D882-18	5
6%MC	6	ASTM D882-18	5
8%MC	8	ASTM D882-18	5
10%MC	10	ASTM D882-18	5